Superlattices of organic/inorganic semiconductor nanostructures from liquid-crystal templates

M. A. Carrasco-Orozco, T. Stirner,* and M. O'Neill
Department of Physics, University of Hull, Hull HU6 7RX, United Kingdom

C. Ellis, D. Dong, R. Kelly, M. O. Piepenbrock, and S. M. Kelly†
Department of Chemistry, University of Hull, Hull HU6 7RX, United Kingdom

(Received 19 May 2006; revised manuscript received 7 November 2006; published 8 January 2007)

A lyotropic liquid-crystal-templated superlattice of inorganic CdSe semiconductor nanostructures within an organic semiconductor polymer-network film was fabricated by a self-assembly process. The film is characterized with small-angle x-ray diffraction experiments and ultraviolet-visible absorption measurements. Empirical pseudopotential calculations of the effective CdSe nanocrystal band gap show that the experimental observations are consistent with the formation of CdSe nanostructures inside lyotropic liquid-crystal nanotubes. A potential application of these nanocomposite supramolecular arrays is demonstrated via a photoconductive device.

DOI: 10.1103/PhysRevB.75.035207 PACS number(s): 72.80.Tm, 72.80.Le, 73.21.Hb, 73.22.Dj

I. INTRODUCTION

The fabrication and characterization of self-assembled nanocomposites and nanoscale materials with novel physical properties for light-emitting and photovoltaic devices has received considerable attention over the past decade.[1–7] Following the initial investigations of Wang and Herron[8] and Dabbousi *et al.*[9] of quantum-dot polymer composites, Greenham *et al.*[10] were the first to report experiments involving the conjugated polymer MEH-PPV poly(2-methoxy-5-(2′-ethylhexyloxy)-*p*-phenylenevinylene) intermixed with spherical CdS or CdSe nanoparticles. Photovoltaic devices fabricated from this blend showed an efficiency that improved when the amount of CdSe was increased, leading to the conclusion that electron transport limited the device performance. It was demonstrated later by Huynh *et al.*[11] that elongated, rodlike CdSe nanocrystals embedded in poly-3(hexylthiophene) improve the device efficiency as the rods tend to form directed chains creating defined pathways for electron transport to the appropriate electrode, with first devices achieving external quantum efficiencies of up to 16%. These same authors subsequently tuned the nanocrystal dimensions to change the distance over which electrons are transported directly through the device and to optimize the overlap between the absorption spectrum of the solar cell and the solar emission spectrum, giving rise to external quantum efficiencies of over 54% and power conversion efficiencies of 1.7% under AM 1.5 global solar conditions.[12] An alternative method of fabricating nanocomposites was put forward by Gin and co-workers.[13,14] These researchers generated a reversed hexagonal phase from a lyotropic liquid crystal and proposed to use the water cores of the ensuing structure for the inclusion of water-soluble luminescent molecules such as PPV. The degree of PPV conversion was monitored via fluorescence spectroscopy, and a blueshift of the fluorescence of the nanocomposite with respect to bulk PPV was observed. The nanocomposites also gave rise to an increase in photoluminescence per unit volume compared to pure PPV which was attributed to a decrease in self-quenching mechanisms.[13] This fabrication method was later also employed to incorporate silicates[15] and CdS[16] into the water core channels.

In this paper, we present a method of fabricating a superlattice array of inorganic CdSe semiconductor nanostructures within an organic liquid-crystal semiconductor polymer network as a thin plastic film. This organized organic/inorganic hybrid supramolecular structure may be used for a range of electro-optic applications such as photovoltaic devices.

II. EXPERIMENT

The method of synthesis is modified from the literature,[13,14] but uses a new monomer shown in Fig. 1 to form a lyotropic liquid crystal. The aromatic core of **1** should exhibit a low ionization potential and is designed as a hole-transport element. Synthetic details will be reported elsewhere. When mixed with water, the photopolymerizable amphiphile molecules self-assemble into a reversed hexagonal phase (H_{II} phase) by forming a matrix around the water cores. Experiments[14] have shown that the H_{II} phase and, in particular, the diameter of the water core channels are relatively insensitive to variations in temperature. This is consistent with a packing model of the monomer molecules within which the phenyl rings of the monomer units are stacked above each other, forming disks that enclose the water channels—i.e., the formation of an organic "nanotube" array. Photopolymerization of the lyotropic liquid crystal ensures that the organic film becomes insoluble and the alignment is retained indefinitely. The presence of reactive agents in the water channels—e.g., in the form of transition-metal ions at the hydrophilic end of the monomers—may lead to the formation of composites when water-soluble "filler" materials flow through the channels. Hence, the fabrication of organic-template-inorganic-semiconductor nanocomposites can be achieved. The advantage of the present fabrication method is that the polymerized columnar liquid-crystalline state generates and maintains architectural control of the nanocomposite as well as passivating and preventing lateral agglomeration of the inorganic semiconductor nanostructures. The regular arrangement of the electron-transporting semiconductor nanostructures into a well-defined superlattice oriented perpendicular to the electrodes, shown schematically in Fig. 2,

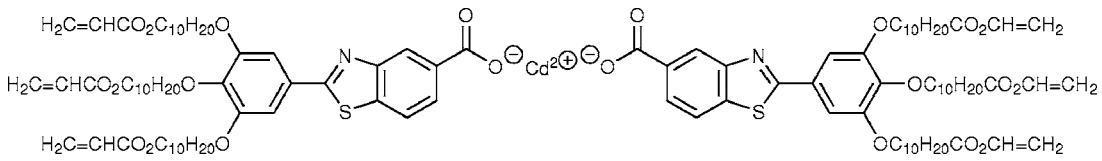

FIG. 1. Molecular structure of the lyotropic liquid crystal **1**.

combined with a hole-transporting liquid-crystalline polymer matrix, should prevent the trapping of charge carriers at dead ends in the nanocomposite, thus facilitating the fabrication of highly efficient and robust photovoltaic cells. In addition, nanocrystals made from inorganic semiconductors are also considered to be a promising way towards hybrid organic/inorganic light-emitting devices.[10]

In the present experiments, the H_{II} phase is formed by adding some water to the Cd-salt—i.e., the amphiphile shown in Fig. 1. We prepare a homogeneous mixture under nitrogen atmosphere, which has a texture similar to toothpaste. Although we found that 8 wt % of water is sufficient to fully hydrate our sample and to obtain the required reversed hexagonal phase, several combinations with different water content were tried, confirming that the reversed hexagonal phase is present up to 20 wt % water.[14] We note, however, that the stability of the H_{II} phase is increasingly compromised for higher water content, and consequently the fraction of water in the mixture was kept close to the minimum required. Similarly, 8 wt % of water was found to be too small to prepare well-mixed solutions. Hence, xylene was added (up to 10 wt % of the amphiphile) to help dissolve the Cd-salt. The addition of xylene gives a three-phase mixture forming the lyotropic liquid crystal. It lowers the viscosity and improves the spreadability of the paste, both essential features for materials processing. The components were manually mixed and then deposited in a hermetically closed container. The sample was placed in an ultrasonic bath for 20 min and then mixed in a centrifuge for 30 min. A second sonification completed the paste preparation procedure. The paste was left to rest for some time, usually overnight, before films were prepared without any sign of decomposition or phase separation. To prepare the film for characterization, a small amount of lyotropic paste was taken from the main container and placed on top of a clean quartz slide (sometimes ITO glass was used). Another quartz-glass slide was placed on top of the first one in order to form a sandwich and to transmit the UV radiation required for the photopolymerization process. The sandwich was placed on top of a hot plate and heated just beyond the clearing point (90 °C). Constant, uniform pressure was applied to the sandwich in order to obtain a homeotropic alignment of the lyotropic liquid crystal and the concomitant formation of nanotubes (schematically illustrated in Fig. 2). Optical microscopy of the sample between crossed polarizers (not shown) provided evidence of a uniform, homeotropic alignment of the film.

The 367-nm line of a 100-W high-pressure mercury arc lamp was employed to polymerize the film. A fluence of 50 J cm^{-2} is required for full polymerization. The presence of six polymerizable acrylate end groups per monomer ensures a high cross-link density. After completion of the photopolymerization process, the sample is exposed to H_2Se gas. The H_2Se dissolves in water, diffuses through the water channels, and reacts with the Cd ions on the inside of the nanotubes—i.e., $H_2Se + CdX_2 \rightarrow CdSe + 2HX$, where X represents the hydrophobic end of the amphiphile; i.e., the free carboxilic acid is formed.

III. RESULTS AND DISCUSSION

Standard small-angle x-ray diffraction (SAXD) measurements were used to confirm the formation of the H_{II} phase. The measurements were carried out using a Siemens D5000 diffractometer ($\lambda = 1.54$ Å) on films deposited on a polished Si substrate. A hexagonal arrangement of columns gives rise

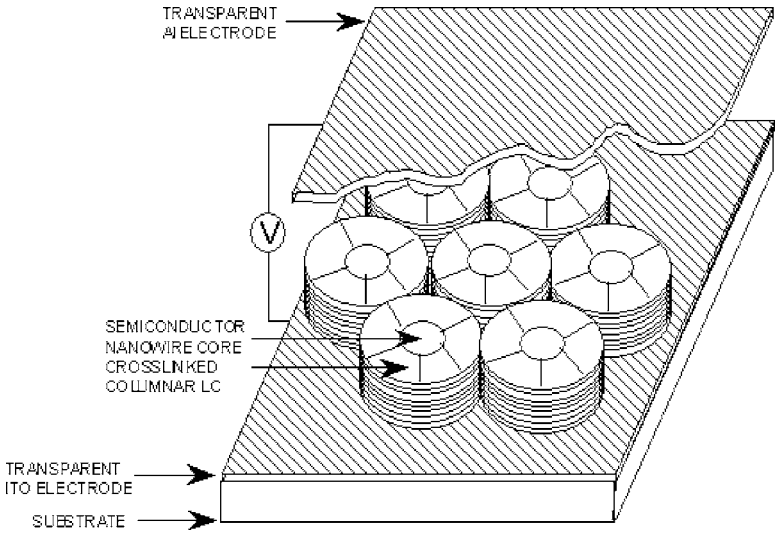

FIG. 2. Schematic diagram of the photoconductive device architecture lyotropic liquid crystal–CdSe nanocrystal supramolecular array sandwiched between an ITO/quartz-glass substrate and aluminum cathode. The lyotropic liquid crystal forms a hexagonal, columnar H_{II} phase with the CdSe nanocrystals being located inside the central water channels. Polymerization chemically bonds the columns to form a thin organic semiconductor polymer network with a regular array of inorganic CdSe semiconductor nanostructures embedded in the film. The film is mechanically robust and can be removed without tearing.

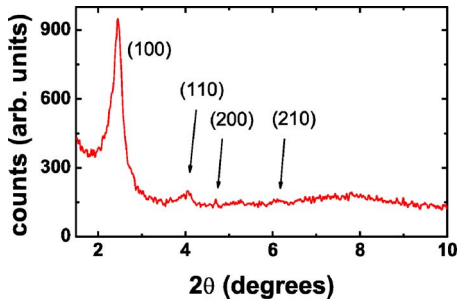

FIG. 3. (Color online) Small-angle x-ray diffraction spectrum of the photopolymerized lyotropic liquid-crystal film. The theoretical diffraction peak positions for a hexagonal structure arising from diffraction on the planes (*hkl*) are indicated by arrows.

to a characteristic set of interplanar d spacings following the sequence $1:1/\sqrt{3}:1/\sqrt{4}:1/\sqrt{7}\ldots$ and the Bragg equation was utilized to determine the dimensions of the lattice from the diffraction peaks. The observed d spacings of $d_{10}=36.0$ Å, $d_{11}=21.7$ Å, $d_{20}=18.8$ Å, and $d_{21}=14.2$ Å (after polymerization[17]) are in agreement with the above sequence (see Fig. 3) to within an error of less than 5%. This confirms that the lyotropic liquid crystal forms a two-dimensional reversed hexagonal lattice which is also retained after photopolymerization.[15] From the spacings of the x-ray diffraction planes it is also possible to calculate the lattice constant using the geometric relationship $2r=\sqrt{4/3}d_{10}$ (see Fig. 4). Using the observed d_{10} spacing in this expression gives a value of $2r=41.6$ Å. Tate and Gruner[18] derive an equation for the diameter of the water core channels (d_w) as a function of water content (ϕ_w) in the channels—i.e., $d_w=2(2r)\sqrt{\phi_w\sqrt{3}/2\pi}$. Using the above lattice constant $2r$ and the known water content in the system of $\phi_w=8\%$ gives a diameter of the water channels of $d_w=12.4$ Å.

Ultraviolet-visible (UV-vis) spectroscopy was used to monitor the change in absorbance of the lyotropic liquid-crystal film on exposure to H_2Se. Any change in the absorption spectrum points to a variation in the composition of the film due to the precipitation of CdSe. In particular, if the formation of CdSe nanostructures occurs, we would expect an increase in absorbance at wavelengths shorter than 719 nm—i.e., an absorption edge that is blueshifted with respect to bulk CdSe due to quantum confinement effects. A computer-controlled UV-vis spectrometer (Aurora Scan, Unicam 5625) was used for the absorbance measurements. The spectral range is 200–1100 nm, with 2-nm resolution, using a combination of deuterium and tungsten lamps. Figure 5 shows the spectrum of the unexposed film as well as the spectra after exposure of the film to H_2Se for 3 and 6 days, respectively. The spectra can be deconvoluted into two separate components—i.e., an intense peak centered at around 344 nm originating from the organic template and a less intense band at wavelengths between approximately 400 and 550 nm. As can be seen from Fig. 5, the less intense band is absent for the unexposed film and grows with increasing exposure of the sample to the H_2Se gas. Consequently, we attribute this band to the formation of CdSe nanocrystals inside the lyotropic liquid crystal nanotubes. The absorbance continues to increase with increasing exposure time up to approximately 6 days, after which saturation occurs. This observation is consistent with a diffusion-limited process, such as the diffusion of H_2Se through the water channels. If we assume that the diffusion length σ of this process is approximately equal to the film thickness L (with $L=5$ μm), we arrive at a diffusion coefficient for H_2Se through the water channels of $D=\sigma^2/2t\approx 10^{-17}$ m^2 s^{-1}. This value is considerably lower than typical diffusion coefficients of small molecules in water ($\sim 10^{-9}$ m^2 s^{-1}, Ref. 19), which we attribute to the small dimensions of the water channels impeding the Brownian motion of H_2Se.

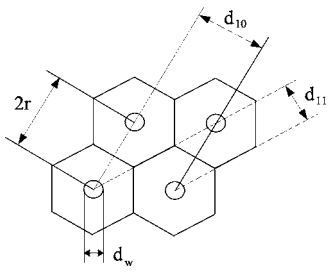

FIG. 4. Schematic diagram of the Wigner-Seitz unit cell for the H_{II} phase showing the lattice constant $2r$, the diameter of the water core channels d_w, and the first two x-ray diffraction planes d_{10} ($h=1$, $k=0$) and d_{11} ($h=1$, $k=1$).

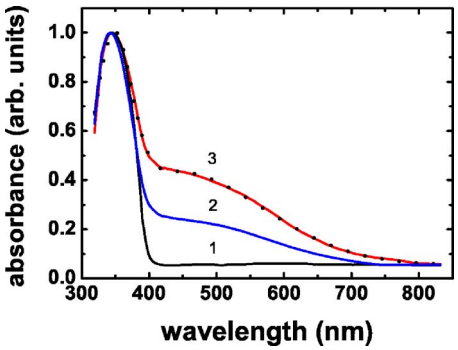

FIG. 5. (Color online) UV-vis absorption spectra of a thin film of homeotropically aligned **1** in the H_{II} phase (normalized at 344 nm) before (1) and after exposures to H_2Se for 3 days (2) and 6 days (3). The dotted line represents the best fit to curve (3) with two Gaussians.

As well as providing a method to monitor the formation of CdSe, the UV-vis peak absorption energy can also be compared to theoretical calculations of electronic transition energies. Since the transition energy depends on the size (size distribution) and shape of the nanostructures, such calculations allow insight into the structural details of the CdSe nanocrystals. In order to obtain the experimental transition energy, we fit the UV-vis absorption spectrum with two Gaussians. The result of this fitting procedure is shown by the dotted line in Fig. 5 and gives a value of ≈441 nm (or 2.81 eV) for the center of the absorption peak associated with the CdSe nanocrystals. We have carried out computer simulations of the electronic energy band structure of CdSe employing the empirical pseudopotential method[20–23] within the single-band truncated-crystal approximation.[24] Details of this method can be found in Refs. 22 and 25. The empirical

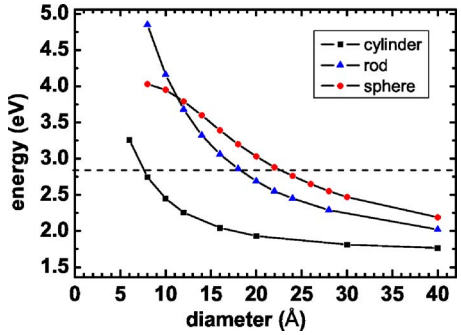

FIG. 6. (Color online) Calculated effective CdSe bandgap for nanocylinders (■), nanorods (▲), and nanospheres (●) using the empirical pseudopotential method [the lines are to guide the eye only; the calculations for the CdSe nanospheres are in good agreement with experimental data available in the literature (Ref. 28)]. The horizontal dashed line indicates the experimental peak transition energy associated with the CdSe nanocrystals.

pseudopotential form factors for zinc-blende CdSe were taken from Ref. 26. The spin-orbit interaction is included using a model described by Bloom and Bergstresser.[27] Here 169 plane waves are used in the calculations to converge the eigenenergies to an accuracy of ~1 meV. The simulations were carried out for three different geometries: namely, nanospheres, nanorods, and nanocylinders. For nanospheres of radius R the electron wave vector, projected onto each Cartesian axis with equal magnitude, is given by

$$\mathbf{k} = \frac{\pi}{\sqrt{3}R}(n_x, n_y, n_z), \tag{1}$$

where n are the quantum numbers of the particle. For nanorods of radius R the electron wave vector, projected onto each of the two Cartesian axes perpendicular to the nanorod axis z, is given by

$$\mathbf{k} = \frac{\alpha_0}{\sqrt{2}R}(n_x, n_y), \tag{2}$$

where $\alpha_0 = 2.4048$ is the first zero of the Bessel function, while for nanocylinders of radius R the electron wave vector is described by

$$\mathbf{k} = \frac{1}{\sqrt{2}R}(n_x, n_y). \tag{3}$$

The calculated effective band gaps for these three geometries are plotted in Fig. 6 as a function of sphere, rod, or cylinder diameter, respectively. The experimental peak absorption energy for the CdSe nanostructures is also indicated in this figure by the dashed horizontal line. As can be seen, in order to give agreement with the observed transition energy of 2.81 eV, the *nanospheres* would have to have a diameter of ≈23 Å, while the *nanorod* diameter would need to be ≈18 Å. Both of these values are larger than the diameter of the nanotubes of ≈12 Å (determined independently via the SAXD measurements described above). However, if we assume a *nanocylinder* geometry for CdSe in the calculations, we arrive at a cylinder diameter of ≈8 Å, which is in good

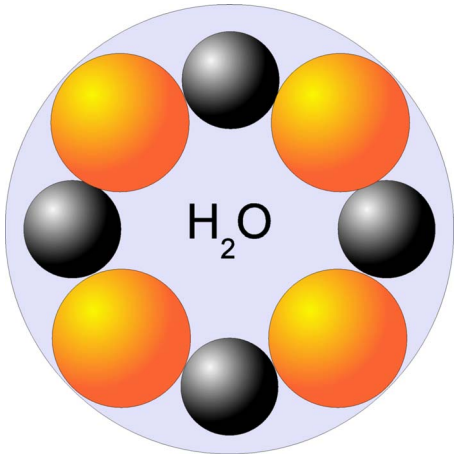

FIG. 7. (Color online) Schematic diagram (cross-section) of a CdSe nanocylinder inside a lyotropic liquid-crystal nanotube (water core channel). The diagram is drawn approximately to scale using the ionic radii of Cd^{2+} (dark gray) and Se^{2-} (orange/light gray). On this same scale a water molecule is approximately the size of the H_2O symbol.

agreement with the observed water channel diameter. Consequently, we argue that the reaction of H_2Se with the Cd amphiphile monomers is consistent with the formation of CdSe nanocylinders inside the lyotropic liquid crystal nanotubes. A possible arrangement of the Cd and Se atoms forming a nanocylinder of single monolayer thickness inside a water-channel nanotube is shown schematically in Fig. 7. Nevertheless, we cannot exclude completely the formation of other crystal geometries for the following reasons: (i) uncertainties in the actual confinement of the charge carriers, (ii) a relatively broad absorption band indicating large size fluctuations and/or geometry variations of the CdSe nanocrystals, and (iii) the possibility of a deformation of the pores during the formation of the CdSe. The present calculations are limited by the assumption of an infinite potential, and closer agreement with experimental results would be expected if the actual confinement of the electrons and holes were considered. This is not possible without a free parameter, since the band alignments between the conduction and valence bands of the semiconductor and the lowest unoccupied and

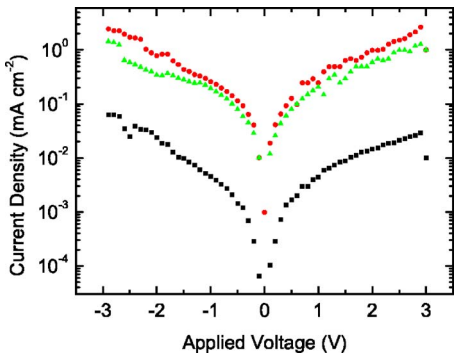

FIG. 8. (Color online) Current-voltage characteristics of the photoconductive device (see Fig. 2) in the dark (■), on irradiation with light of wavelength 480 nm and intensity 0.23 mW cm^{-2} (●), and following removal of the incident light (▲).

highest occupied molecular orbital (LUMO and HOMO) energies of the lyotropic three-phase mixture are unknown.

A photoconductive device was made by sandwiching the inorganic/organic superlattice between ITO and Al electrodes (see Fig. 2). Figure 8 shows the dark current and photocurrent versus voltage characteristics of the device. A quantum efficiency of 2.6% was obtained at an applied voltage of −1 V on irradiation with light of wavelength 480 nm and intensity 0.23 mW cm^{-2}. No photovoltaic effect was found, as expected, since the device incorporated no carrier-blocking layers. Figure 8 also shows that the photoconductivity is persistent and has a half-life greater than a half hour. There are many examples of persistent photoconductivity in semiconductors,[29,30] where the barrier to current injection at the electrodes is changed by the population of long-lived traps. Similarly, in ZnCdSe it has been shown that compositional fluctuations can lead to random local potential wells trapping charge.[31] A similar effect may operate here. Potential wells may result from the formation of nonuniform cylinders, leading to long-lived traps and/or percolation states.

IV. CONCLUSIONS

In summary, we have successfully fabricated a regular superlattice of inorganic CdSe semiconductor nanostructures in an organic semiconductor polymer-network film by a lyotropic liquid-crystalline templating process. The present nanocomposite films can be used as a different approach to photovoltaic devices. The potential of these hybrid organic/inorganic semiconductors in other electrooptic applications is significant—e.g., as a different approach to photonic band gap media. The present method employs photopolymerization, and consequently there is potential for lithographic patterning of these supramolecular arrays.

ACKNOWLEDGMENT

We thank the EPSRC U.K. (Grant No. GR/N65943/01) for financial support.

*Electronic address: t.stirner@hull.ac.uk
†Electronic address: s.m.kelly@hull.ac.uk

[1] J. H. Golden, F. J. DiSalvo, J. M. J. Fréchet, J. Silcox, M. Thomas, and J. Elman, Science **273**, 782 (1996).
[2] P. V. Braun, P. Osenar, and S. I. Stupp, Nature (London) **380**, 325 (1996).
[3] P. Osenar, P. V. Braun, and S. I. Stupp, Adv. Mater. (Weinheim, Ger.) **8**, 1022 (1996).
[4] P. Calvert and P. Rieke, Chem. Mater. **8**, 1715 (1996).
[5] J. Hagen, W. Schaffrath, P. Otschik, R. Fink, A. Bacher, H. W. Schmidt, and D. Haarer, Synth. Met. **89**, 215 (1997).
[6] S. Kumar and T. Nann, J. Mater. Res. **11**, 2220 (2004).
[7] Y. Lin, A. Böker, J. He, K. Sill, H. Xiang, C. Abetz, X. Li, J. Wang, T. Emrick, S. Long, Q. Wang, A. Balazs, and T. P. Russell, Nature (London) **434**, 55 (2005).
[8] Y. Wang and N. Herron, Chem. Phys. Lett. **200**, 71 (1992).
[9] B. O. Dabbousi, M. G. Bawendi, O. Onitsuka, and M. F. Rubner, Appl. Phys. Lett. **66**, 1316 (1995).
[10] N. C. Greenham, X. Peng, and A. P. Alivisatos, Phys. Rev. B **54**, 17628 (1996).
[11] W. U. Huynh, X. Peng, and A. P. Alivisatos, Adv. Mater. (Weinheim, Ger.) **11**, 923 (1999).
[12] W. U. Huynh, J. J. Dittmer, and A. P. Alivisatos, Science **295**, 2425 (2002).
[13] R. C. Smith, W. M. Fischer, and D. L. Gin, J. Am. Chem. Soc. **119**, 4092 (1997).
[14] R. Resel, U. Theissl, C. Gadermaier, E. Zojer, M. Kriechbaum, H. Amenitsch, D. Gin, R. Smith, and G. Leising, Liq. Cryst. **27**, 407 (2000).
[15] D. H. Gray, S. L. Hu, E. Juang, and D. L. Gin, Adv. Mater. (Weinheim, Ger.) **9**, 731 (1997).
[16] D. H. Gray and D. L. Gin, Chem. Mater. **10**, 1827 (1998).
[17] We observe a small decrease in the unit cell dimensions of the hexagonal mesophase upon polymerization. The interplanar spacings before polymerization are d_{10}=36.6 Å, d_{11}=22.3 Å, d_{20}=19.2 Å, and d_{21}=14.2 Å.
[18] M. W. Tate and S. M. Gruner, Biochemistry **28**, 4245 (1989).
[19] P. W. Atkins, *Physical Chemistry* (Freeman, New York, 1996).
[20] M. L. Cohen and T. K. Bergstresser, Phys. Rev. **141**, 789 (1966).
[21] L.-W. Wang and A. Zunger, J. Phys. Chem. **98**, 2158 (1994).
[22] T. Stirner, N. T. Kirkman, L. May, C. Ellis, J. E. Nicholls, S. M. Kelly, M. O'Neill, and J. H. C. Hogg, J. Nanosci. Nanotechnol. **1**, 451 (2001).
[23] T. Stirner, J. Chem. Phys. **117**, 6715 (2002).
[24] M. V. Rama Krishna and R. A. Friesner, J. Chem. Phys. **95**, 8309 (1991).
[25] S. M. Kelly, M. O'Neill, and T. Stirner, in *Handbook of Electroluminescent Materials*, edited by D. R. Vij (IOP, Bristol, 2004), Chap. 4.
[26] F. Long, Ph.D. thesis, University of Hull, 2000.
[27] S. Bloom and T. K. Bergstresser, Solid State Commun. **6**, 465 (1968).
[28] A. Tomasulo and M. V. Ramakrishna, J. Chem. Phys. **105**, 3612 (1991).
[29] O. Katz, G. Bahir, and J. Salzman, Appl. Phys. Lett. **84**, 4092 (2004).
[30] D. Seghier and H. P. Gislason, J. Phys. D **32**, 369 (1999).
[31] H. X. Jiang and J. Y. Lin, Phys. Rev. B **40**, 10025 (1989).